15TH IEA HEAT PUMP CONFERENCE
MAY 26–29, 2026 | HOFBURG
VIENNA 2026
DECARBONISATION THROUGH INNOVATION

Heat transfer characteristics of low-GWP refrigerants in a smooth horizontal tube

Amal Vasu[a], Young Soo Chang[b]

[a]Department of Mechanical Engineering, Graduate School, Kookmin University: Seoul, 02707, Korea
[b] School of Mechanical Engineering, Kookmin University: Seoul, 02707, Korea

Abstract

Understanding the heat transfer characteristics of refrigerants is essential for the design and optimization of heat exchangers. In this study, the heat transfer characteristics of low-GWP refrigerants R454C, R455A and a ternary refrigerant blend R32[19.1], R1234yf[56.7], CF3I[24.2] is experimentally investigated in a horizontal tube. Several evaporation heat transfer correlations were evaluated to assess their predictive accuracy against the experimental data. Among the correlations examined, those proposed by Shah (2015), mixture corrected-Liu and Winterton (1991), and Kim and Mudawar (2013) showed the best overall performance, exhibiting the lowest mean absolute deviations relative to the measurements. The Kim and Mudawar (2013) correlation provided the highest accuracy, with a mean absolute deviation percentage of 13.9% and a mean relative deviation percentage of 3.4%.

Keywords: Low-GWP refrigerants; Evaporation heat transfer coefficient; Correlation assessment

1. Introduction

The transition toward environmentally sustainable cooling and heating technologies have accelerated the adoption of refrigerants with low global warming potential (GWP). As international regulations continue to restrict the use of high-GWP fluids, considerable attention has shifted to refrigerants such as R455A, R454C, and new refrigerant blends. These mixtures offer not only substantially lower GWP values but also practical advantages in terms of safety, material compatibility, and suitability for use in existing refrigeration and heat-pump systems.

R454C is a binary zeotropic mixture of R32/R1234yf (21.5/78.5 wt%) with a low global warming potential (GWP = 148), making it a long-term replacement for R404A. Its moderate temperature glide of approximately 4.2 K and similar thermophysical characteristics to R404A enable drop-in applicability with minimal system modification[1]. Several studies have evaluated R454C as a drop-in replacement for R404A, reporting improved COP up to 10% higher, primarily due to reduced compressor power consumption, despite a slight reduction in cooling capacity[1].

R455A has emerged as a promising long-term replacement for R404A in commercial refrigeration systems, unlike interim blends such as R448A, R449A, and R452A, whose relatively high GWPs limit their future applicability[2-5]. Recent evaluations show that R455A can provide comparable or improved performance, with vapor-compression tests reporting COP gains of around 10% relative to R404A[6] and system-level studies confirming similar behavior in low-temperature applications [7]. Simulation-based assessments further indicate that although R455A and R454C exhibit lower heat-transfer coefficients than R410A, they remain viable candidates from an environmental and performance standpoint[8-9]. In addition, Berto et al. [10] experimentally investigated the flow boiling heat transfer of the zeotropic mixture R455A in horizontal smooth tubes and demonstrated that its significant temperature glide influences both nucleate and convective boiling mechanisms, requiring modified correlations to account for mass transfer resistance.

* Corresponding author. *E-mail address:* yschang@kookmin.ac.kr

A notable feature of these blends is their temperature glide, which can significantly influence phase-change heat-transfer behavior. Glides affect the local driving temperature difference during evaporation and may alter the dominant heat-transfer mechanisms compared with traditional pure refrigerants. As a result, accurately predicting evaporation performance becomes essential for the proper design and optimization of heat exchangers.

Although many evaporation heat-transfer correlations are available in the literature, most were originally developed for conventional refrigerants or mixtures with modest temperature glide. As a result, their performance for newer low-GWP blends has not been extensively examined, mainly due to the limited amount of experimental data currently available for these refrigerants. In this context, the present study focuses on evaluating the predictive accuracy of commonly used evaporation heat-transfer correlations when applied to R454C, R455A, and the R32/R1234yf/CF_3I ternary blend. Using experimental measurements obtained across various operating conditions, the study aims to determine which existing correlations offer reliable performance and to identify their limitations when used with these modern low-GWP refrigerants.

Accordingly, this work investigates the heat transfer performance of R454C, R455A, and the R32/R1234yf/CF_3I ternary blend and compares the experimental data with several widely used evaporation heat-transfer correlations.

2. Methodology

The experimental setup used to measure the evaporation heat transfer coefficient (HTC) under various operating conditions is shown in Fig. 1. The experimental setup consists of a plate-type heat exchanger, liquid receiver, subcooler, refrigerant pump, Coriolis mass flow meter, pre-heater, pressure transducers, temperature sensors, and a data acquisition system. The test section is a 1-m-long horizontal smooth copper tube with an inner diameter of 4.6 mm. An absolute pressure transducer is mounted at the test-section inlet, while a differential pressure sensor measures the pressure drop across the tube. Pt100 RTDs are installed directly in the refrigerant line at both the inlet and outlet of the test section, with the sensing tips in direct contact with the refrigerant stream to ensure accurate temperature measurements.

To determine the evaporation heat-transfer coefficient, wall-temperature measurements were taken at three axial locations, 25 cm, 50 cm, and 75 cm, from the inlet of the 1-m heated test section (positions A, B, and C). At each position, four Type-T thermocouples were mounted evenly around the tube's outer circumference to capture the local wall temperature distribution. Refrigerant evaporation within the test section was driven by an electric heater. A uniform heat flux was achieved by tightly winding nichrome wire around the copper tube, with the supplied heat precisely regulated through voltage control. The electrical power delivered to the heater was monitored using a power meter. The vapor quality at the inlet of the test section was adjusted by varying the AC current supplied to the preheater.

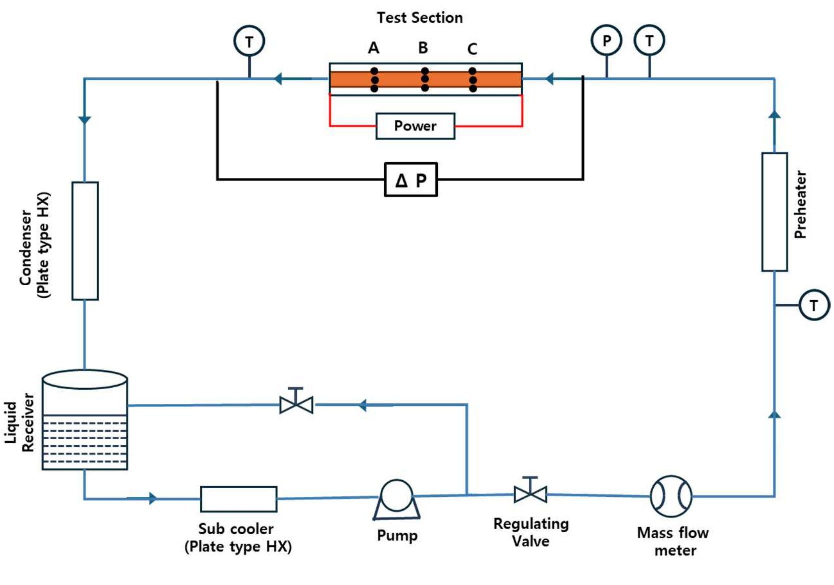

Figure 1. Evaporation measurement experimental set up.

The tests were conducted with mass flux ranging from 200 to 400 kg/(m²·s), heat flux from 10 to 20 kW/m², and saturation temperatures between −10 and 10 °C. Details of the experimental setup are provided in our previous work [11]. All experiments were conducted under steady-state conditions. Steady state was assumed to be reached when the monitored parameters, including inlet and outlet refrigerant temperatures, saturation pressure, mass flow rate, and electrical heat input, remained within ±1% of their mean values for a minimum duration of 10 minutes. Data acquisition was initiated only after this steady-state condition was confirmed.

2.1. Data reduction

The evaporation heat transfer coefficient at test section is determined using Eq. (1), where q is the heat flux determined using Eq. (2), T_{wi} is the inner wall temperature, T_{ref} is the refrigerant temperature determined by taking the average of refrigerant temperature measured at the inlet and outlet of test section using Eq. (3).

$$HTC = \frac{q}{T_{wi} - T_{ref}} \tag{1}$$

$$q = \frac{Q}{\pi d_i L} \tag{2}$$

$$T_{ref} = \frac{T_{ref\ in} + T_{ref\ out}}{2} \tag{3}$$

$$T_{wi} = T_{wo} - \frac{Q_{test} \ln \frac{d_o}{d_i}}{2\pi k L} \tag{4}$$

$$T_{wo} = \frac{T_{woA} + T_{woB} + T_{woC}}{3} \tag{5}$$

$$x = \frac{i_{average} - i_f}{i_{fg}} \tag{6}$$

$$i_{outlet} = i_{inlet} + \frac{Q_{test}}{\dot{m}} \tag{7}$$

$$i_{inlet} = i_{pre,inlet} + \frac{Q_{pre}}{\dot{m}} \tag{8}$$

Inner wall temperature T_{wi} is calculated using the steady-state heat conduction equation, Eq. (4), assuming one-dimensional radial heat transfer. The outer wall temperature is obtained from Eq. (5) by averaging the wall temperature measured at locations *A*, *B* & *C* along the test section, which are spaced 25 cm apart. At each axial location (A, B, and C), the wall temperature was obtained by averaging the readings of the four circumferentially distributed thermocouples. Although the refrigerants exhibit temperature glide, the measured wall temperatures at locations A, B, and C showed only small axial variations compared to the wall–fluid temperature difference used to calculate the heat transfer coefficient. Therefore, the use of an average wall temperature is considered appropriate.

The representative vapor quality of the test section was determined based on the average refrigerant enthalpy calculated from the inlet and outlet values from Eqs. (6)-(8), where i_f is the saturated liquid enthalpy and i_{fg} is the latent heat of vaporization corresponding to the refrigerant pressure.

The refrigerant enthalpy at the measurement location is determined by Eq. (7), where $\mathrm{i_{inlet}}$ is the enthalpy at the test section inlet, which is determined by energy balance in the pre-heater using Eq. (8). All thermodynamic properties are calculated using REFPROP 10.0[12].

2.2. Uncertainty Analysis

Experimental uncertainties were evaluated based on instrument specifications (Table 1), while uncertainties of derived parameters were estimated using standard error propagation methods (Moffat, 1988[13]). The resulting maximum uncertainties of the main parameters are summarized in Table 2. The dominant source of uncertainty in the heat transfer coefficient was the wall–refrigerant temperature difference; as reported by Hoang et al. (2022) [14], smaller temperature differences at high mass flux and high HTC conditions lead to increased uncertainty. Accordingly, the HTC uncertainty ranged from 7.1% under average conditions to a maximum of 12.3%.

Table 1. Instrument and sensor accuracy

Parameter	Range	Accuracy
Temperature (Pt100 RTDs)	-80 – 250 ℃	±0.05° C
Wall temperature (T-type Thermocouples)	5-85 ℃	±0.3° C
Absolute Pressure sensor (Full scale)	4000 kPa	±0.11 %
Differential pressure (Full scale)	68.9 kPa	±0.172 kPa
Coriolis mass flow meter	0.4 -2 8kg/min	±0.2 %

Table 2. Maximum value of uncertainty

Parameter	Maximum uncertainty
Mass flux	± 3.6 $kg/s{\cdot}m^2$ (0.9 %)
Heat flux	± 0.22 kW/m^2 (1.1 %)
Vapor quality	± 0.012
HTC	± 0.16 $kW/m^2.K$ (7.1%) - ± 0.48 $kW/m^2.K$ (12.3%)

3. Heat transfer coefficient variation

The heat transfer coefficient was measured for the refrigerants R454C, R455A, and the blend R32 [19.1%], R1234yf [56.7%], and CF_3I [24.2%] over the experimental range summarized in Table 3

Table 3. Test conditions

Parameter	Range
Mass flux ($kg/s.m^2$)	200-400
Heat flux (kW/m^2)	10-20
Vapor quality	0.1-0.9
Temperature (average of bubble and dew) in the test section (°C)	-10-10

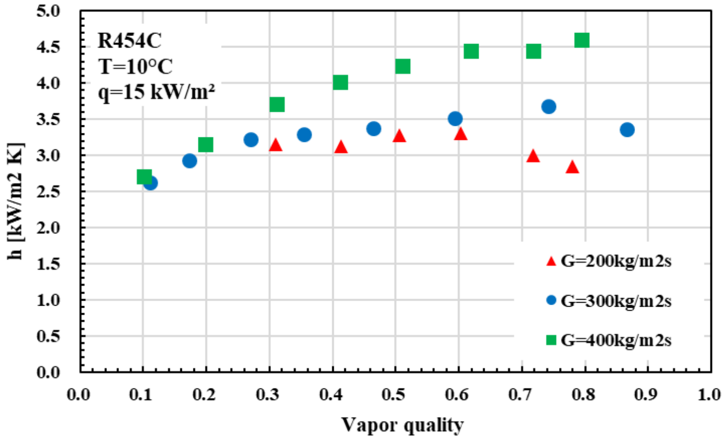

(a) R454C

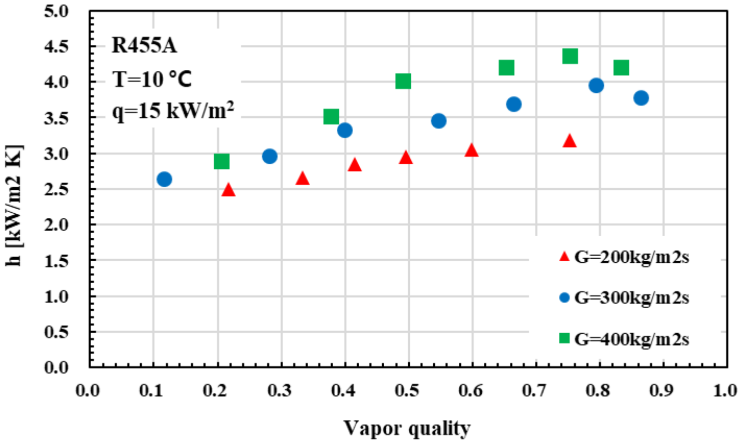

(b) R455A

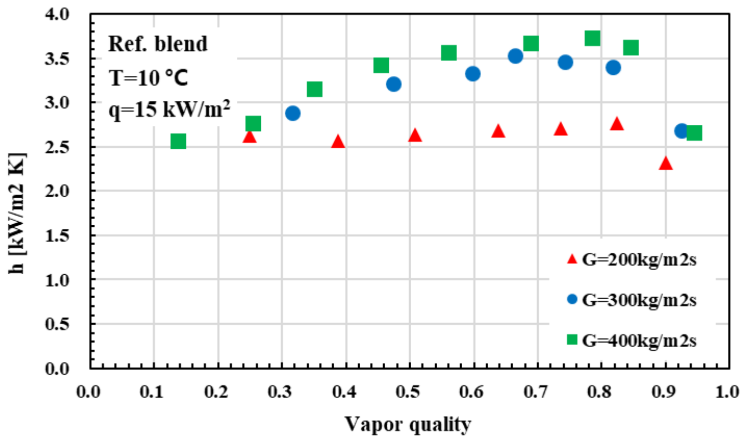

(c) Refrigerant blend R32[19.1], R1234yf[56.7], CF3I[24.2]

Figure 2. Measured heat transfer coefficients at various conditions.

Fig. 2 presents the measured heat transfer coefficients of the tested refrigerants under various operating conditions. Fig. 2(a) illustrates how the HTC of R454C varies with mass flux at an evaporation temperature of 10 °C and a heat flux of 15 kW/m². At low vapor qualities, the HTC remains nearly unchanged regardless of mass flux. However, at higher vapor qualities, the HTC increases noticeably with increasing mass flux. This behavior suggests that convective heat transfer becomes increasingly dominant at higher vapor qualities, where increased mass flux enhances vapor shear and liquid film disturbance, leading to improved heat transfer.

Fig. 2(b) illustrates the heat transfer behavior of R455A at an evaporation temperature of 10 °C and a heat flux of 15 kW/m². The heat transfer coefficient increases with vapor quality at a heat flux of 15 kW/m², indicating an increasing contribution of convective boiling as the vapor phase becomes dominant. In addition, higher mass flux consistently enhances the HTC over the entire vapor quality range. For example, increasing the mass flux from 200 to 400 kg/(m²·s) results in an HTC increase of approximately 31% at a vapor quality of 0.3 and about 38% at a vapor quality of 0.7. This trend reflects the stronger convective heat transfer associated with higher mass velocities, which is consistent with the behavior reported by Choi et al. (2025)[15].

Fig. 2(c) shows the heat transfer coefficients of the refrigerant blend under the same conditions (T = 10 °C, q = 15 kW/m²). The heat transfer coefficient exhibits a weak dependence on vapor quality at the lowest mass flux of 200 kg/(m²·s), suggesting a weaker role of convective effects, which is often reported when nucleate boiling contributes significantly to heat transfer. At higher mass fluxes, the HTC increases but shows only modest differences between 300 and 400 kg/(m²·s), indicating a reduced rate of enhancement as convective boiling becomes dominant and further increases in mass flux provide diminishing benefits.

4. Evaluation of correlations against present experimental data

The experimentally measured HTCs for the tested low-GWP refrigerants were used to evaluate the predictive performance of several existing correlations. A total of 320 data points were included in the analysis. The prediction accuracy was quantified using Eq. (9) and Eq. (10), where MADP denotes the mean absolute deviation percentage and MRDP represents the mean relative deviation percentage. Fig. 3 presents the HTC predictions obtained from the various evaporation models.

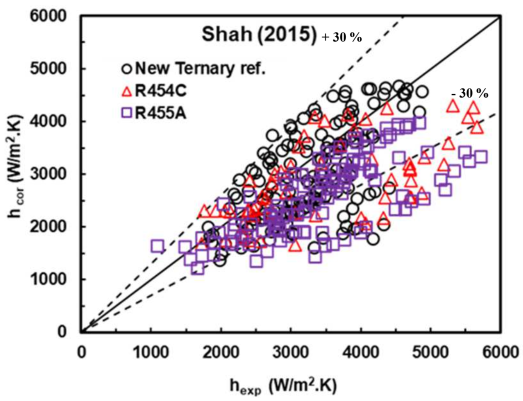

(a) Shah (2015) [16]

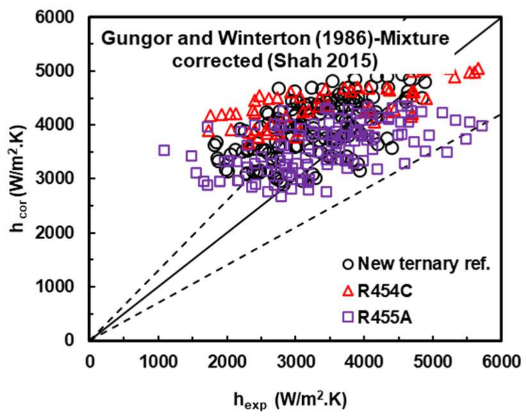

(b) Gungor and Winterton (1986) [17]

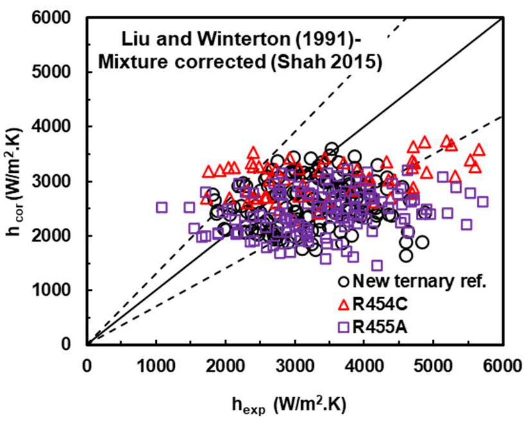

(c) Liu and Winterton (1991)[18]

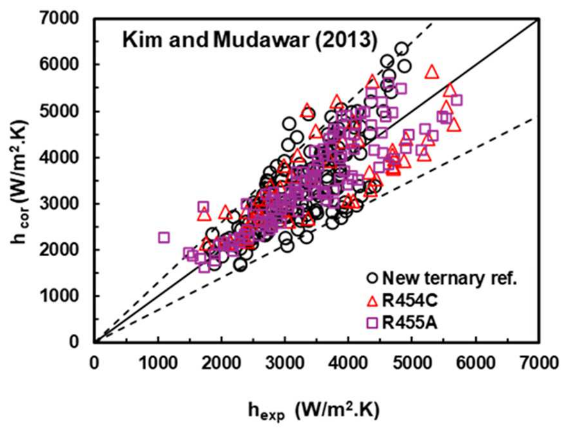

(d) Kim and Mudawar (2013) [19,20]

Figure 3. Heat transfer coefficient prediction

Fig. 3 (a) shows the prediction with Shah, 2015 [16] model. The Shah (2015) correlation includes mixture effects through the use of the Thome–Shakir correction for nucleate boiling and the Bell–Ghaly method for convective boiling, which account for mass transfer resistance associated with temperature glide in zeotropic refrigerants. Most data points lie close to zero deviation line, indicating reasonable agreement, although a noticeable scatter exists, particularly at higher HTC values. The new ternary refrigerant shows the best agreement with the line of perfect prediction, whereas R454C and R455A deviate more, mainly due to underprediction. The Shah correlation generally follows the experimental trend, with noticeable underprediction at higher HTC values.

The mixture-corrected Gungor and Winterton (1986) [17] model shows overprediction (Fig. 3(b)), particularly at lower heat transfer coefficient (HTC) values. This overprediction is more evident for R454C and less for R455A, suggesting that the model tends to overestimate heat transfer under weak boiling conditions. Since R454C has a lower temperature glide than the other tested refrigerants, the applied glide correction is smaller, whereas the higher-glide refrigerant R455A experiences a stronger correction that reduces the apparent overprediction.

Fig. 3(c) shows a comparison between the experimental HTCs and the predictions from the mixture-corrected Liu and Winterton (1991) [18] correlation. This model tends to underpredict the data, and its predictive trend is inferior to that of Shah (2015).

Fig. 3(d) shows the performance of the Kim and Mudawar (2013) [19,20] correlation. Compared with the other correlations, the predicted values align more closely with the line of perfect agreement, for all three refrigerants tested. A similar trend has also been reported in a previous study [11] involving a high-glide refrigerant blend. Overall, the Kim and Mudawar (2013) correlation provides the most consistent and accurate predictions among the evaluated models for the present experimental dataset. The prediction accuracy of all correlations is further illustrated in Fig. 4 and Table 4.

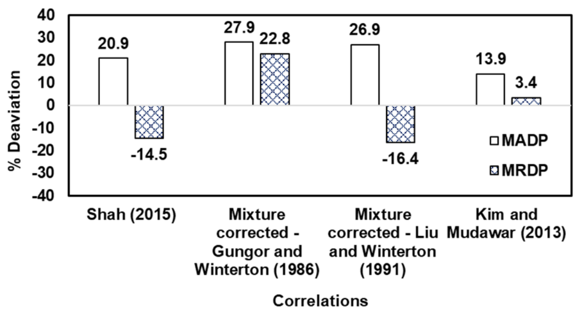

Figure 4. Overall prediction accuracy

Table 4. Prediction accuracy

Correlation	MADP (%)	MRDP (%)
Shah (2015)	20.9	-14.5
Mixture corrected- Gungor and Winterton (1986)	27.9	22.8
Mixture corrected- Liu and Winterton (1991)	26.9	-16.4
Kim and Mudawar (2013)	13.9	3.4

5. Conclusion

This study examined the evaporation heat transfer behavior of low-GWP refrigerants R454C, R455A, and a new ternary blend, and compared the measurements with several widely used correlations. Shah (2015) and Kim and Mudawar (2013) captured the general trends reasonably well, whereas the mixture-corrected Gungor and Winterton (1986) model consistently overpredicted the data, and the mixture-corrected Liu and Winterton (1991) model underpredicted the data. Among all the models evaluated, the Kim and Mudawar (2013) correlation showed the closest match to the experimental results, giving the lowest deviation for all refrigerants tested. These results suggest that the Kim and Mudawar (2013) model is the most reliable option for predicting evaporation heat transfer for the low-GWP refrigerants considered, offering practical guidance for the design and optimization of heat exchangers using next-generation refrigerant blends.

Acknowledgements

This work was supported by Korea Institute of Energy Technology Evaluation and Planning (KETEP) grant funded by the Korean government (MOTIE, RS-2024–00432255, Development of eco-friendly low-temperature cold chain refrigeration system technology in response to refrigerant regulations).

References

[1] Arcasi, A., Mauro, A.W., Napoli, G., Viscito, L., 2022. Heat transfer coefficient, pressure drop and dry-out vapor quality of R454C: Flow boiling experiments and assessment of methods. International Journal of Heat and Mass Transfer 188, 122599.

[2] Lillo, G., Mastrullo, R., Mauro, A.W., Viscito, L., 2018. Flow boiling data of R452A. Energy Procedia 148, 1034–1041.

[3] Lillo, G., Mastrullo, R., Mauro, A.W., Pelella, F., Viscito, L., 2019. Experimental thermal and hydraulic characterization of R448A and comparison with R404A during flow boiling. Applied Thermal Engineering 161, 114146.

[4] Kim, C.-H., Kim, N.-H., 2021. Evaporation heat transfer and pressure drop of interim (R448A, R449A) and long-term (R455A, R454C) low-GWP R404A alternatives in a smooth tube. International Journal of Heat and Mass Transfer 181, 121903.

[5] Kedzierski, M.A., Kang, D., 2016. Horizontal convective boiling of R448A, R449A and R452B within a micro-fin tube. Science and Technology for the Built Environment 22, 1175–1184.

[6] Mota-Babiloni, A., Haro-Ortuño, J., Navarro-Esbrí, J., Barragán-Cervera, A., 2018. Experimental drop-in replacement of R404A for warm countries using the low-GWP mixtures R454C and R455A. International Journal of Refrigeration 91, 136–145.

[7] Sethi, A., Pottker, G., Yana-Motta, S., 2016. Experimental evaluation and field trial of low-global-warming-potential R404A replacements for commercial refrigeration. Science and Technology for the Built Environment 22, 1175–1184.

[8] Mauro, A.W., Napoli, G., Pelella, F., Viscito, L., 2020. Flow boiling heat transfer and pressure drop data of non-azeotropic mixture R455A in a horizontal 6.0 mm stainless-steel tube. International Journal of Refrigeration 119, 195–205.

[9] Vasu, A., Chang, Y.S., 2025a. Performance simulation of the indoor unit of a heat pump with low-GWP alternative refrigerants. Journal of Mechanical Science and Technology 39(2), 997–1007.

[10] Berto, A., Azzolin, M., Bortolin, S., Guzzardi, C., Del Col, D., 2020. Measurements and modelling of R455A and R452B flow boiling heat transfer inside channels. International Journal of Refrigeration 120, 271–284.

[11] Vasu, A., Chang, Y.S., 2026. Evaporation heat transfer correlation for CF_3I/R1132a refrigerant blend in a horizontal tube. Journal of Mechanical Science and Technology 40(1).

[12] Lemmon, E.W., Bell, I.H., Huber, M.L., McLinden, M.O., 2018. NIST Standard Reference Database 23: Reference Fluid Thermodynamic and Transport Properties (REFPROP), Version 10.0. National Institute of Standards and Technology, Gaithersburg.

[13] Moffat, R.J., 1988. Describing the uncertainties in experimental results. Experimental Thermal and Fluid Science 1, 3–17.

[14] Hoang, H.N., Agustiarini, N., Oh, J.T., 2022. Experimental investigation of two-phase flow boiling heat transfer coefficient and pressure drop of R448A inside multiport mini-channel tube. Energies 15(12).

[15] Choi, Y., Vasu, A., Ahn, J., Chang, Y.S., 2025. Flow boiling heat transfer and pressure drop of R455A in a horizontal smooth tube. Journal of Thermal Science and Technology 20(2).

[16] Shah, M.M., 2015. A method for predicting heat transfer during boiling of mixtures in plain tubes. Applied Thermal Engineering 89, 812–821.

[17] Gungor, K.E., Winterton, R.H.S., 1986. A general correlation for flow boiling in tubes and annuli. International Journal of Heat and Mass Transfer 29(3), 351–358.

[18] Liu, Z., Winterton, R.H.S., 1991. A general correlation for saturated and subcooled flow boiling in tubes and annuli, based on a nucleate pool boiling equation. International Journal of Heat and Mass Transfer 34, 2759–2766.

[19] Kim, S.M., Mudawar, I., 2013. Universal approach to predicting saturated flow boiling heat transfer in mini/micro-channels – Part I: Dryout incipience quality. International Journal of Heat and Mass Transfer 64, 1226–1238.

[20] S. M. Kim and I. Mudawar.,2013. Universal approach to predicting saturated flow boiling heat transfer in mini/micro-channels – Part II: Two-phase heat transfer coefficient. International Journal of Heat and Mass Transfer 64, 1239–1256.